Heliyon 8 (2022) e09128

Contents lists available at ScienceDirect

Heliyon

journal homepage: www.cell.com/heliyon

Research article

Lytic cocktail: An effective method to alleviate severe burn induced hyper-metabolism through regulating white adipose tissue browning

Meng Zhang [a,b,1], Peilang Yang [a,1], Tianyi Yu [a], Martin C. Harmsen [b], Min Gao [a], Dan Liu [a], Yan Shi [a], Yan Liu [a,**], Xiong Zhang [a,*]

[a] Department of Burn, Ruijin Hospital, Shanghai Jiao Tong University School of Medicine, 200025, China
[b] University of Groningen, University Medical Center Groningen, Department of Pathology and Medical Biology, Hanzeplein 1 (EA11), 9713GZ Groningen, the Netherlands

ARTICLE INFO

Keywords:
Server burn induced-hypermetabolism
Lytic cocktail
White adipose tissue browning
Uncoupling protein 1 (UCP1)

ABSTRACT

Background: Browning of white adipose tissue is associated with elevated resting metabolic rates and is considered to be one of the indispensable causes of hypermetabolism in burn patients. Hypermetabolism means increased resting energy expenditure, raised body temperature and acute-phase proteins. Persistently elevated levels of circulating stress hormones have been reported to induce browning of subcutaneous white adipose tissue. The lytic cocktail is a combination of medicines pethidine, chlorpromazine, and promethazine that has been used clinically in sedation for the management of patients. As reported this sedative treatment can reduce the expression of catecholamines in major burn rats. Thus, in this paper we focused on the effects of lytic cocktail in the regulation of white adipose tissue browning and hypermetabolism and we further investigated the underlying mechanism.

Methods: A 30% total body surface area (TBSA) III degree scald rat model was used for this study. The rats were randomly divided into a sham scald group, a scalding with immediate resuscitation group, and a group of scalding with immediate resuscitation and lytic cocktail treatment. The levels of norepinephrine and epinephrine in plasma were dynamically detected. Changes of the rat body weight and food intake were recorded and compared as indexes of metabolism responses after post-scalding. For the study of white adipose tissue browning, inguinal adipose tissue was used. Metabolic changes, while indicatives of white fat browning were measured by PET/CT. The expression of white adipose browning related proteins and the changes of mitochondria number were used to assess browning of inguinal adipose.

Results: The level of plasma catecholamines norepinephrine and epinephrine in the lytic cocktail-treated group was significantly lower than the other two groups. Morphology and PET/CT showed that the inguinal white adipose browning was inhibited in the lytic cocktail treated group, whereas scalding with immediate resuscitation group showed browning of white adipose. The number of mitochondria, the expressions of white adipose browning related proteins in the lytic cocktail group were also significantly lower than that of the group of scalding with immediate resuscitation.

Conclusion: By reducing expression of heat-related proteins, the application of lytic cocktail medicines inhibits the white adipose tissue browning, which suppresses hypermetabolism in scalded rats. The mechanism might be related to decreased expression levels of stress hormones induced by lytic cocktail. This research suggests that lytic cocktails may be an effective treatment for hypermetabolism after severe burn injury.

1. Introduction

Hypermetabolism, which defined as an elevated resting energy expenditure (REE) above 110% of predicted REE [1], is a remarkable metabolic consequence of severe burns. These responses include increasing in REE, raising body temperature and acute-phase protein response. The high expression of catecholamines together with other neuron endocrine hormones such as renin-angiotensin and

* Corresponding author.
** Corresponding author.
E-mail addresses: rjliuyan@126.com (Y. Liu), xiong@medmail.com.cn (X. Zhang).
[1] These authors contributed equally to this work.

https://doi.org/10.1016/j.heliyon.2022.e09128
Received 8 September 2021; Received in revised form 28 December 2021; Accepted 14 March 2022

adrenocorticotropic hormone are widely considered as key factors that lead to the hypermetabolic responses of burn injuries with total body surface area (TBSA) exceeding 30% [2]. William et al has found that significant increase in catecholamine levels was detected in the children's urine samples at 11–20 days after severe burns [3]. Hypermetabolism induced by severe burn comprises significant catabolism, insulin resistance with hyperglycemia and lipolysis. Moreover, it culminates in delayed wound healing and a compromised immune system function which coincides with increased infections, sepsis multiorgan failure and death [4, 5]. It is reported that the burn-induced hypermetabolism may persist for as long as 24 months [1]. The proper management of hypermetabolic states is crucial in treating major burn patients [6, 7].

In the 1950s, a French military doctor Henri Laborit created an artificial hibernation, a treatment of a Lytic cocktail medicine, to attenuate and block excessive neuroendocrine reactions in severe trauma patients. The Lytic cocktail consists of pethidine, chlorpromazine, promethazine mixed in a ratio of 2:1:1 [8]. Pethidine is an opioid analgesic with a large range of central nervous system inhibitory effects, including decreased level of serum cortisol [9]. The sedative effect of pethidine is greatly enhanced when combined with chlorpromazine and promethazine. This sedative treatment has been approved to lower body temperature and reduce the basal metabolic rates [10] as well as dampen the stress hormone levels caused by severe trauma. It has been used intramuscularly for the burn patient's management as a sedative treatment for many years in Ruijin Hospital. Previous studies have revealed that the administration of lytic cocktails could reduce the expression of stress hormones such as catecholamines [11] and protect organ function in severely scalded rats [12]. The pathophysiologic mechanism of such regulation, however, still needs to be explored in more details.

In recent years researchers found that subcutaneous white adipose tissue (sWAT) possessed similar characteristics to brown adipose tissue (BAT) in severely burned humans and animals [13, 14]. In rodent, BAT mostly exists in interscapular, subscapular, axillary, perisubclavian and pericarotid, visceral depots deposit in the cervical spine, mediastinum, pericardium and perirenal [15, 16]. For human, BAT deposit in supraclavicular and neck, paravertebral, mediastinal, para-aortic, and suprarenal areas [17]. Similar to BAT and different from the original white adipocytes such as multilocular lipid droplets, multilocular lipid droplets, the browned sWAT is featured with the presence of multil ocular adipocytes, intensive numbers of mitochondria, and high expression of Uncoupling protein-1 (UCP1) [13, 18]. UCP1 mainly presents in the proton channel in the mitochondrial inner membrane as carrier protein. It could cause short-circuit aerobic metabolism via disruption of the electrochemical gradient. As proton transport fails to establish the necessary electrochemical gradient for ATP synthesis, the chemical energy is converted to heat in browned WAT instead [19]. Analysis of the metabolism after scalding indicated that changing mitochondrial biogenesis including the larger number of mitochondria and increased expression of UCP1 might be one of the indispensable reasons for hypermetabolism [20].

Research have proved that a formation of the sWAT browning is likely to require a prolonged adrenergic stress [21]. It has been published that the levels of catecholamine are raised after burn injury and then decreased with time up to around 100 days [3]. WAT browning is the process of conversion of WAT into beige adipose tissue. This is corroborated by chronically increased catecholamine levels in severe burn patients in which the thermogenic activities of beige adipose tissue are found upregulated [22, 23]. Beige adipose tissue is activated through the β3-AR-PKA-CREB-UCP1 pathway. Catecholamine stimulates the β3 receptor on the cell surface of beige adipose, leading to activation of adenylate cyclase, increased cAMP concentration and enhanced PKA activity. PKA phosphorylates CREB, which in turn activates the expression of peroxisome proliferator-activated receptor gamma coactivator 1-alpha (PGC-1α). PGC-1α is an activating transcription factor that binds to the transcription factor peroxisome proliferator-activated receptor gamma (PPAR-γ) to promote UCP1 expression. *Prdm16* is a zinc finger DNA-binding protein that promotes PGC-1α and PPAR-γ-dependent gene expression by binding to the CCAAT enhancer binding protein β to form a transcriptional complex, to further mediate brown fat cell formation. Studies have shown that subcutaneous fat in mice stimulated by β3 receptor agonists express higher levels of PGC-1α [24].

Since the lytic cocktail treatment could reduce the catecholamine concentration in burn injuries [11], how could such application affect the regulation of the WAT browning process? With this question, we used a 30% TBSA III degree scald rat model to investigate if the lytic cocktail treatment would help to regulate the WAT browning process as well as hypermetabolism and further to understand the mechanisms of such regulation. In this paper, for the first time, we reported that the application of lytic cocktail can inhibit the formation of browning WAT by reducing the expression of adrenaline and noradrenaline. We have also found the evidence that burn-induced hypermetabolism could be reduced through the inhibition of WAT browning.

2. Material and methods

2.1. Animal and experimental model

57 male Sprague-Dawley rats weighing 180–250 g (age 6–8 weeks) were obtained from Shanghai Laboratory Animal Center in the Chinese Academy of Sciences. All the rats were housed at the Animal Science Center of Shanghai Jiao Tong University, School of Medicine (SJTUSM) and cared for according to Guide for the Care and Use of Laboratory Animals and all experiment were approved by the SJTUSM Institutional Animal Care and Use Committee (approval number: B-2016-016).

Following a three-day adjustment period, the rats were divided into three groups randomly: sham-scalding controls (Ctrl, n = 19), scalding with immediate resuscitation (RE, n = 19), and scalding with immediate resuscitation and lytic cocktail treatment (RE + lytic, n = 19). Animals were anesthetized with 30 mg/kg pentobarbital intraperitoneally and the hairs in back were shaved prior to experiments. Control animals were immersed with their backs in water of 37 °C for 20 s. The RE group and RE + lytic group rats received a full thickness thermal injury by immersion with their backs in 92 °C water for 20 s which caused a 30% of TBSA in agreement with the published [22]. Intraperitoneal injection of Ringer's solution (2 mL/kg per 1% TBSA) was applied to the RE and the RE + lytic rats post-scalding. The RE + lytic group was intraperitoneal injected the lytic cocktail mixture with pethidine, chlorpromazine, promethazine in a ratio of 2:1:1 (12 mL/kg) immediately and one more injection 24 h after scalding. The weight of all the rats were measured at week 1, 2, 6 after scalding. The inguinal white adipose tissue (iWAT) was harvested at week 6 after scalding.

2.2. The enzyme-linked immunosorbent assay (ELISA)

The expression level of plasma catecholamines was measured by two hormones, noradrenaline, and adrenaline. Blood samples were collected at 24h, 1 w, 2 w and 6 w after scalding. 1 mL blood sample was collected from the angular vein. Measurements of plasma noradrenaline and adrenaline were performed with a Labor Diagnostical Nord GmbH Adrenaline – Noradrenaline ELISA kit according to the manufacturers' protocols.

2.3. Nuclear imaging and ex vivo tracer distribution

Animals were fasted at least 6 h before undergoing PET. ^{18}F-Fluorodeoxyglucose(^{18}F-FDG) was injected via anesthetized rats' tail vein at week 6 after scalding. The injection dose of ^{18}F-FDG per rat is 5.55 MBq/kg. A 10 - min CT was scanned before the PET scan and the rats were subjected to PET imaging 1 h following an injection. The regions of interest (ROIs) were marked with the CT images guidance. All results were expressed as Standardized Uptake Value maximum (SUVmax). We

quantified BAT activity by the maximum uptake value (SUVmax), SUVmax equals dividing the ROI tracer uptake by the ratio of the injected activity to the body weight.

2.4. Proteomics

The iWAT samples of RE and RE + lytic were grinded into fine powder in liquid nitrogen. The cell powder was added to lysis buffer (8 M urea, 1% Protease Inhibitor Cocktail). The volume was 4 times powder. The mixture centrifuged at 12,000 rpm at 4 °C for 10 min after sonicating (ultrasonic processor (Scientz)) on ice. The supernatant was reserved and applied with 5 mM dithiothreitol for 30 min at 56 °C, then followed by 11 mM iodoacetamide for 15 min at room temperature in the dark. Using 100 mM Tetraethylammonium bromide diluted protein solution until urea concentration less than 2 M. Trypsin was added to the samples at 1:50 trypsin-to-protein mass ratio incubated overnight, and then treated with trypsin again at 1:100 mass ratio for 4 h. The peptides were labeled following the instruction of TMT/Itraq and fractionated by High Performance Liquid Chromatography(HPLC). Then they were dissolved in mobile phase A (0.1% formic acid and 2% acetonitrile). Mobile phase B (0.1% formic acid in 98% acetonitrile): 0–26 min (6–23%), 26–34 min (23–35%), 34–37 min (35–80%), and 37–40 min (80%) to finish a cycle. The flow rate was 400 nL/min on an EASY-nLC 1000 UPLC system.

The peptides were separated HPLC, then ionized by NSI source. The electrospray voltage was set to 2.0 kV. The ions were injected into Q Exactive Plus to obtain mass spectra. The Orbitrap scan range was 400–1500 m/z with 70,000 resolutions for first scan. Then selected peptides by NCE setting as 28% and the fragments were detected in the Orbitrap again in 17,500 resolutions. Automatic gain control (AGC) was set at 5E4. AGC target value is set at 78000 ions/s and the maximum ion injection time at 64 ms.

Gene Ontology (GO) was derived from the UniProt-GOA database (http://www.ebi.ac.uk/GOA/). The system converted the protein ID to UniProt ID for matching the GO ID and retrieved the corresponding information from the UniProt-GOA database. If some identified proteins were not searched in the database, InterProScan would be used to annotate protein's GO functional based on protein sequence alignment method. Those proteins were classified by three categories: biological process, cellular component, and molecular function.

2.5. Histological analysis for adipose tissue

The iWAT was immersed in 4% paraformaldehyde in PBS and embedded in paraffin subsequently. Paraffin blocks were sectioned into 6–7μm thickness for each slide. These slides were stained with hematoxylin and eosin. The histology was evaluated by light microscopy.

2.6. Immunohistochemistry for UCP1 determination

Paraffin-embedded tissue sections were dewaxed in xylene, rehydrated in a graded ethanol series (100%, 97% and 70% of ethanol) and washed in demi water. The slides were heated to 95 °C in sodium citrate buffer (pH 6.0) for 15 min for antigen retrieval. To block endogenous peroxidase, sections were applied with 3% H_2O_2 in PBS for 10 min. The sections were incubated with UCP1 (proteintech) at 1:200 dilution as primary antibody at 4 °C overnight and HRP-labeled secondary antibody (CST, 1:500) at room temperature for 1 h, then stained with diaminobenzidine and hematoxylin. The stained sections were reviewed and scored by two pathologists as follows: Staining number score: Cells with <10% staining or no visible staining were given score as negative staining (−, 1); cells were only 10–49% stained scored as (+, 2); cells with 50–74% positive staining were scored as (++, 3); cells with 75–100% positive staining were scored as (+++, 4). Staining color score: 1 score was given for light-yellow particle, 2 for brown-yellow particle and 3 for brown particle. The final score was defined as staining number score multiplied by staining color score [25].

2.7. Transmission electron microscopy

Using 2.5% glutaraldehyde in sodium cacodylate buffer fixed fresh adipose tissue (cut into $1mm^3$). Using 1% osmium tetroxide at 4 °C made tissue post-fixed, and tissue was embedded in epoxy resin. These ultrathin sections were stained with 0.4% lead citrate. All the sections were reviewed under transmission electron microscope. We counted cross sectioned mitochondria per cell manually in the transmission electron microscope pictures.

2.8. Gene expression analyses

Trizol was used for extraction of total mRNA from the iWAT. Reverse-transcribed to cDNA was synthesized followed protocol of PrimeScript® RT reagent Kit. cDNA samples were mixed SYBR1 Premix Ex Taq (Takara)™ and were subjected to PCR analyses. The primers for the internal control(Tubulin) and other genes are: Tubulin: forward primer: 5'GTAAGAAGCAACACCTCCTCC3', reverse primer: 5'CCATGTTCCAGGCAGTAGAG3'. Prdm16: forward primer: 5' TCC ACA CAG AAG AGC GTG AGT A 3', reverse primer: 5' GCT TGC CAC TGT CGT GAG A 3'. Tmem26: forward primer: 5' ACT CTC GGA ACT TCT TCT GAT 3', reverse primer: 5' GCA GGG TTA TTT CTG ACA TTA T 3'. Creb: forward primer: 5' TTG CCC CTG GAG TTG TTA 3', reverse primer: 5' GCT TCC CTG TTC TTC ATT AGA C 3'. The samples were tested on ABI 7500 Real-Time PCR System: 95 °C, 10 min; 95 °C, 15 s x 40; 62 °C, 1 min.

2.9. Western blot

The tissue was ground in liquid nitrogen. The tissue lysis buffer with protease inhibitor cocktail added to protein powder. The mixture was centrifuged at 12000 rpm for 15min, 4 times. Concentrations of protein were determined by BCA assay. 20 μg protein was separated by 12% or 10% acrylamide SDS-PAGEE, and the band transferred to PVDF membrane and conducted for 60min. The membrane was blocked by 5% non-fat powder milk in TBST and incubated at 4 °C with primary antibody UCP1 (proteintech)、PGC-1α (CST)、PPAR-γ (proteintech) overnight. Then incubated with the secondary antibody for 2 h at room temperature after three times TBST rinsed. Membranes were taken images with enhanced chemiluminescence (Millipore). Relative quantities of protein were compared with Tubulin (proteintech) expression. We use imageJ to measure the pixel density of the UCP1, PPAR-γ and PGC1-α band in each group.

2.10. Statistical analysis

Data is expressed as mean ± SD. All statistical analyses were performed using GraphPad Prism v9.2.0. All data were inspected for outliers using GraphPad built-in function. Elisa data and food intake and weight gain were analyzed with two-way ANOVA. PET/CT data, number of mitochondria per cell, histochemistry data, band density of Western blot and PCR data were analyzed with one way ANOVA and corrected multiple comparisons with Tukey. If $p < 0.05$, differences between each group were considered significant in the corresponding statistical tests.

3. Results

3.1. Lytic cocktail decreases circulating norepinephrine and adrenaline levels

The level of adrenaline and noradrenaline were measured by ELISA in the plasma of three rat groups at 24 h, 1 w, 2 w and 6 w after the scalding (Figure 1A, B). There are significantly increased adrenaline and noradrenaline levels in plasma of both burn injury groups compared to the Ctrl group. The lytic cocktail applied group was observed to decrease the expression levels of these two stress hormones.

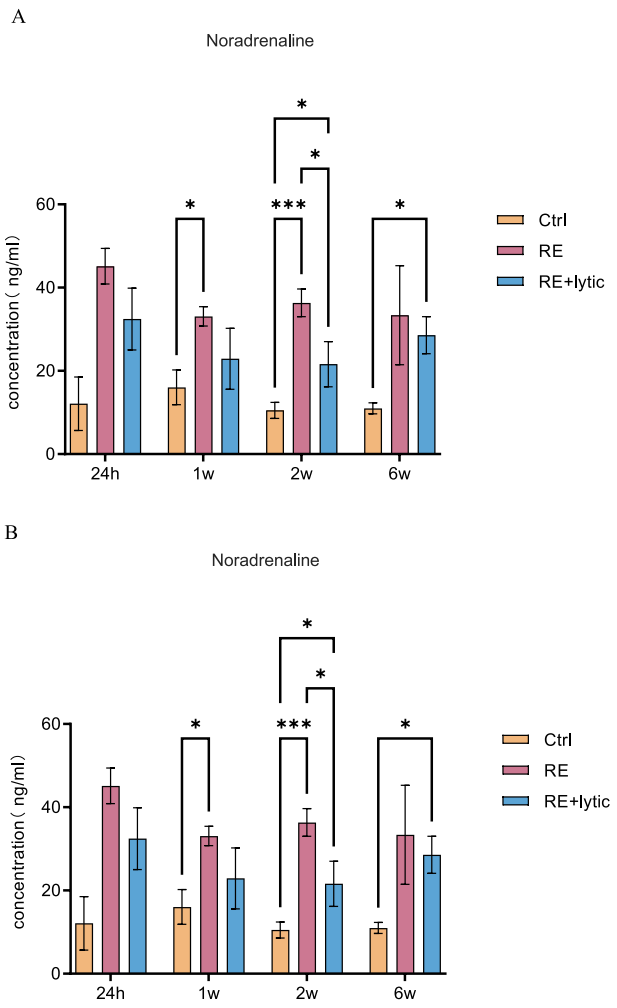

Figure 1. The comparison of norepinephrine and adrenaline expression levels between groups. The level of noradrenaline (A) and adrenaline (B) in the RE + lytic group were both lower than those of the RE group at 24h, 1w, 2w, 6w. Data were obtained from 36 plasma (n = 9), and shown as the mean ± SD, two-way ANOVA comparing norepinephrine and adrenaline in plasma of three group, *p < 0.05, ****p < 0.0001.

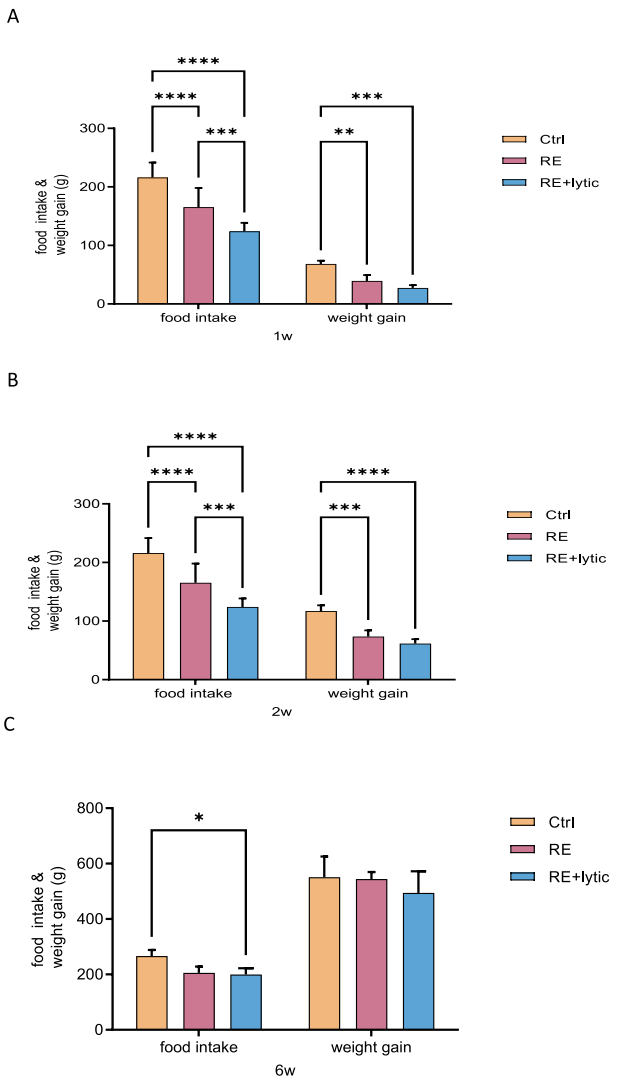

Figure 2. The comparison of metabolic consumptions between groups. The food intake and the body weight were recorded in 1 w (A), 2 w (B) and 6 w (C) after the scalding injury in three groups (n = 7 for each group). The food intake of RE was higher than that of RE + lytic in 1 w and 2 w. The body weight of the RE rats is lower than the RE + lytic group in 2 w after the scalding injury. Data were shown as the means ± SD, two-way ANOVA comparing food intake and the body weight. *p < 0.05, **p < 0.01, ***p < 0.001, ****p < 0.0001.

3.2. Lytic cocktail decreases the energy expenditure of burn rats

The food intake and weight gain of three groups were recorded at 1 w, 2 w, 6 w after the scalding (Figure 2). During the first week, the food intake and weight gain of two burn groups were less in comparison to the Ctrl group ($p < 0.0001$, Figure 2A), which suggested a systemic response was induced by burn injury. However, no significant difference in weight gain was found between RE and RE + lytic at 1 w and 2 w, despite a continuously remarkably diminished food intake in the RE + lytic (Figure 2A, B). These results suggested that lytic cocktail alleviated the condition of high energy consumption. In the final observation of food intake at week 6, the weight gain of the three groups showed no significant difference (Figure 2C).

3.3. Lytic cocktail decreases the metabolism in iWAT of burn rats

Glucose-based uptake visualized with ^{18}FDG-μPET was used to determine the metabolic activity of adipose tissue. iWAT with high uptake are considered hypermetabolic, which indicates the WAT browning. Compared to the Ctrl group, the RE group had increased ^{18}FDG uptake, indicating an increased metabolism and browning of iWAT (Figure 3A). Six weeks after scalding, the functional analysis of iWAT by PET scanning showed that the SUVmax of iWAT in the RE group was 1.97-fold higher than Ctrl group ($p < 0.01$) and 1.78-fold higher than RE + lytic group ($p < 0.01$), Figure 3B). There is no significant difference between the Ctrl and RE + lytic groups. The results indicated that burn injuries increased the metabolism of iWAT and the treatment of lytic cocktails helped to reduce the metabolism and inhibit iWAT from rapid heat generation.

3.4. Lytic cocktail decreases the expression of metabolic proteins and mitochondrial activity

iWAT of the rats in RE and RE + lytic were harvested for proteomics. The quantitative value of each sample was obtained by multiple repeated experiments The differentially expressed proteins were shown by volcano plot (Figure 4A). The differentially expressed protein more than 1.2 was considered significant up-regulation, and less than 1/1.2 for significant down-regulation. After scalding, lytic cocktail upregulated expression of 110 proteins and downregulated 58 proteins compared to scalding only. The differentially expressed proteins are statistically

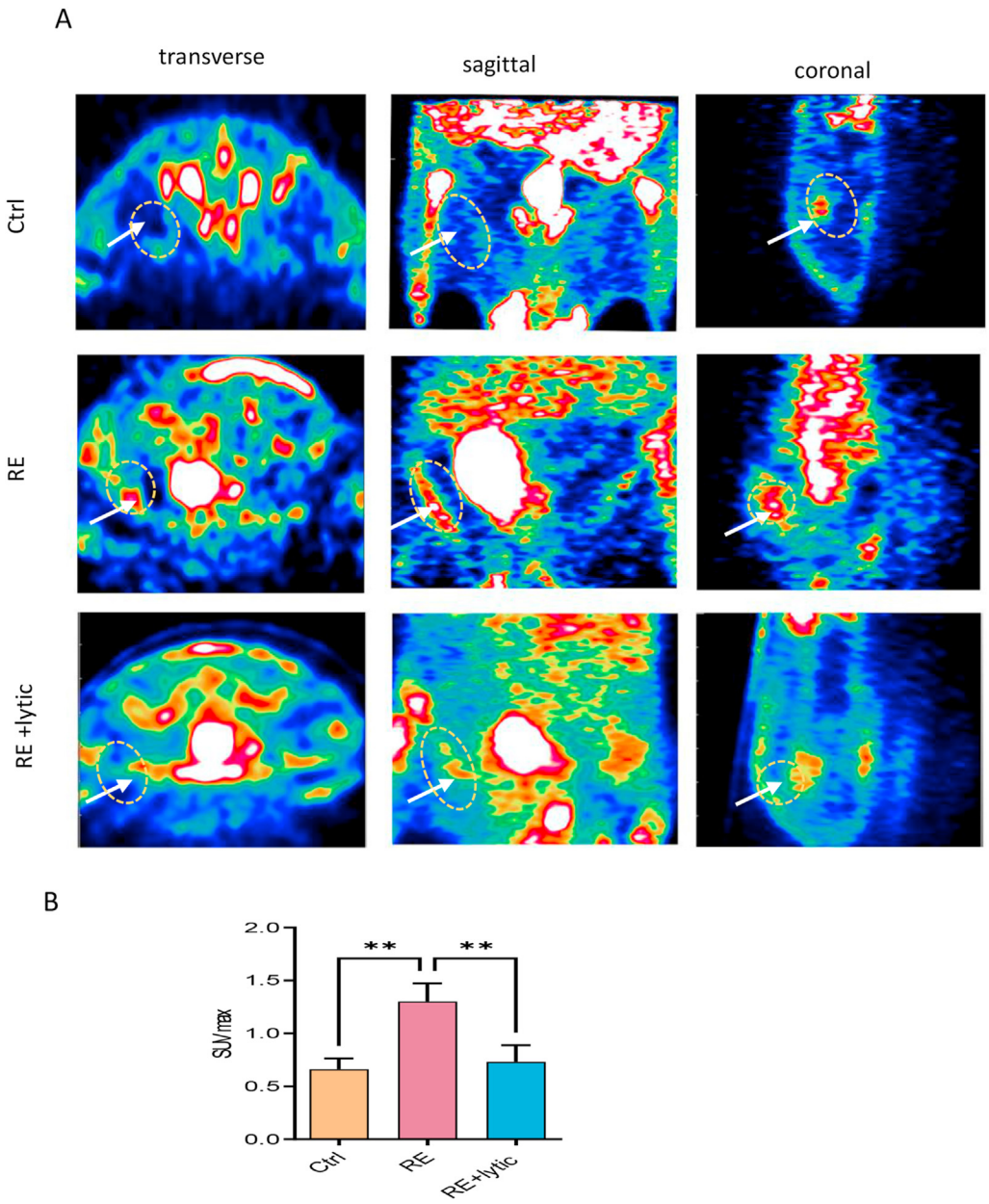

Figure 3. The comparison of metabolism of the iWAT between groups. (A): Representative PET image of 18FDG showed metabolism of the iWAT in Ctrl, RE and RE + lytic, which helped to determine the hypermetabolism in inguinal region (white arrows). The metabolism in inguinal region of RE was much higher than that of Ctrl and RE + lytic. (B): SUV max in three groups demonstrated that uptake of ^{18}FDG in iWAT of RE group increased 2.4 times than that of Ctrl group. Lytic cocktail reduced uptake of ^{18} FDG in iWAT compared to the scalded rats in RE. n = 3 in each group. Data were represented as means ± SD, one-way ANOVA comparing SUV max. **p < 0.01.

classified for their subcellular structure location (Figure 4B). There are 17.24% differentiate proteins located in mitochondria in the RE + lytic group, which indicates that the energy metabolism process is modified by lytic cocktail. Furthermore, 12% increased differentially expressed protein refers to the metabolism process after lytic cocktail treatment (Figure 4C) and 19% decreased differentially expressed proteins refers to the metabolism process (Figure 4D). For differentially expressed proteins, we defined 4 distinct groups in the proteins according to RE + lytic/RE differential expression multiples (Figure 4E). The down-regulated proteins after using lytic cocktail in group Q1 contain 34 types of proteins, and the upregulated proteins after using lytic cocktail in group Q4 contain 91 proteins. We categorized the differential protein enrichment into three (Biological Process, Cellular Component, and Molecular Function) in the GO classification (Figure 4F). Also, we drawn a heat map of molecular function (Figure 4G). The horizontal represents the enrichment test results of different groups, and the vertical is functional enrichment cluster on molecular. It showed hormone receptor binding protein and nuclear hormone receptor binding protein has significant differences after using lytic cocktail.

3.5. Lytic cocktail treatment may reduce histological and molecular browning of iWAT after burn injury

Histological analyses (H&E staining) were used to assess iWAT activation after burn injuries and the impact of lytic cocktail on scalded rats at a microscopic level. In the RE group, white and brown adipocytes coexisted in the browning of iWAT. Multiple and smaller fat vacuoles occupying most of the cell space and a nucleus surrounded by cytoplasms were the two most prominent features of the adipocytes (Figure 5A). In the RE + lytic group, there were less cytoplasm around the adipose droplets; the size of the fat droplet in the RE + lytic group was much smaller than that of the multilobular fat vacuoles seen in the RE group; and the nuclei were continuously found in the peripheral of cells. Such morphology of adipose tissue of lytic cocktail-treated rats demonstrated that the lytic cocktail may inhibit the iWAT browning process.

The ultrastructure of browning adipocytes was observed in the Ctrl rats. There were fat droplets filled up most of adipose cytoplasm and small, rounded mitochondria were scattered in cytoplasm in the Ctrl group (Figure 5B). In contrast, fat droplets in the RE group were smaller.

A

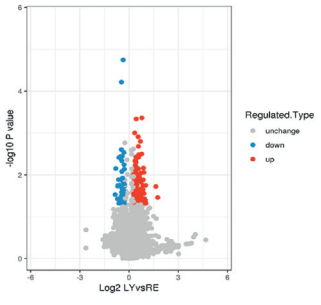

B

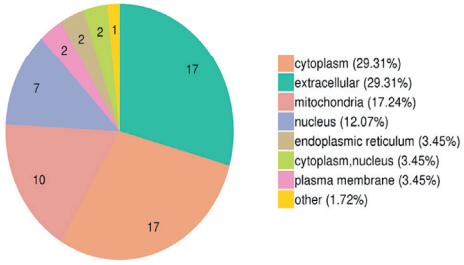

C

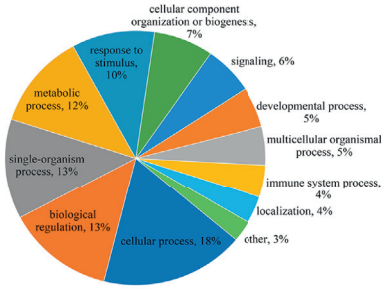

D

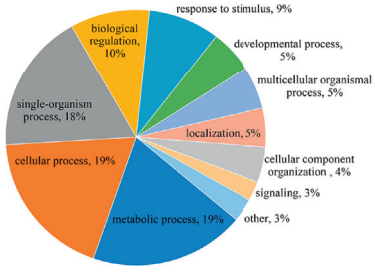

E

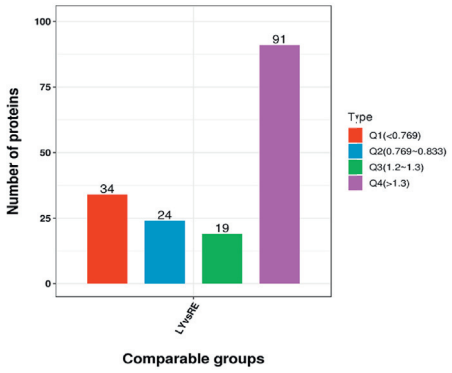

F

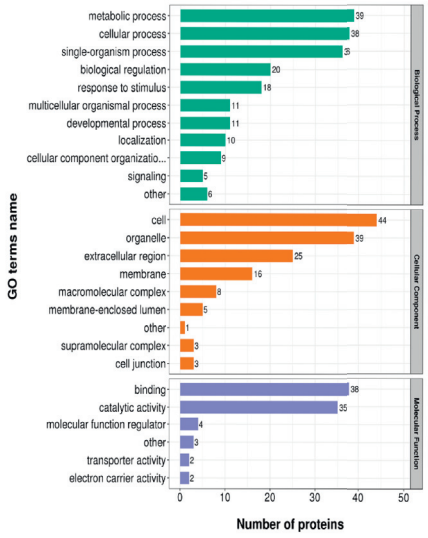

G

(caption on next page)

Figure 4. The expression of metabolic proteins and mitochondrial activity in three groups. (A): The horizontal axis is relative protein quantification value after Log2 logarithmic conversion. The vertical axis is p-value for significance of difference test after the -Log10 logarithmic conversion. The volcano plots showed that significantly differentially expressed up (red) and down (blue) - regulated proteins. (B): The differentially expressed proteins are statistically classified for their subcellular structure location and displayed in different colors. (C): Up-regulated proteins in mitochondria after lytic cocktail treatment. (D): Down-regulated proteins in mitochondria after lytic cocktail treatment. (E): Divided differential proteins into 4 parts according to their differential expression multiples, Q1 means the ratio of differential proteins expression of RE + lytic/RE is less than 0.769. Q2 means the ratio of differential proteins expression of RE + lytic/RE is more than 0.769 but less than 0.833. Q3 means the ratio of differential proteins expression of RE + lytic/RE is more than 1.2 but less than 1.3. Q4 means the ratio of differential proteins expression of RE + lytic/RE is more than 1.3. (F): GO annotation of differential protein in three major categories (Biological Process, Cellular Component, and Molecular Function). (G): Differential protein enrichment analysis of molecular function.

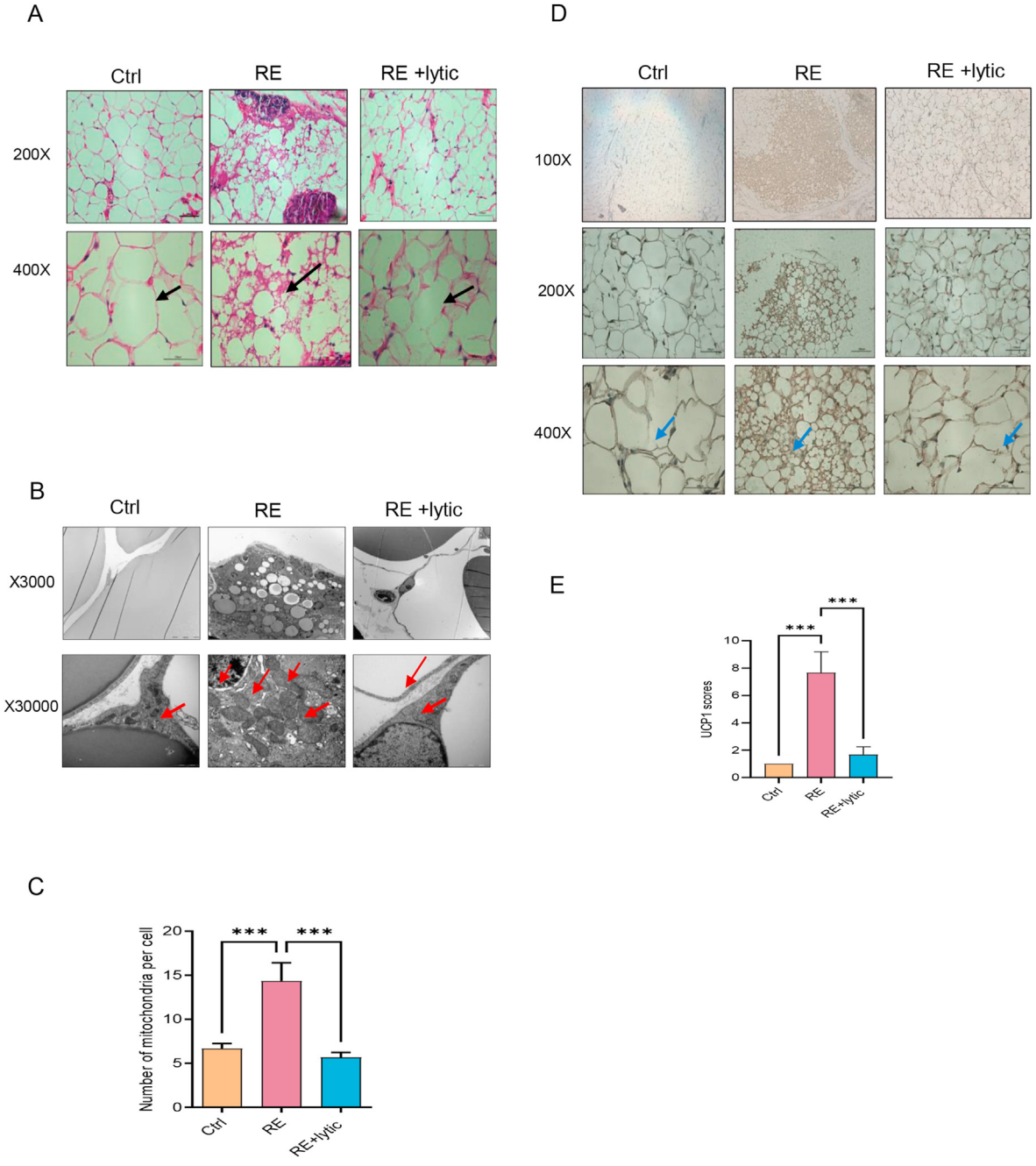

Figure 5. The morphological change of iWAT between groups. (A): H&E staining of iWAT. Morphological change after burn injury and population reduction of white adipocyte were observed in the RE group and lytic cocktail could effectively reduce the consumption of the white adipose (black arrows). A total of nine animals were studied. (B): Transmission electron microscopic of iWAT. iWAT in the RE group showed density decreased of fat droplets in cytoplasm and increased numbers of mitochondria per cell compared to the Ctrl group and the above process could be reversed by lytic cocktail in the RE + lytic group (red arrows). (C): The number of mitochondria per cell in three groups. Data were represented as means ± SD, n = 3 in each group, one-way ANOVA comparing number of mitochondria, ***$p < 0.001$. (D): Immunohistochemistry staining of uncoupling protein-1 (UCP1) in iWAT. UCP1 expression in RE significantly increased compared to Ctrl, and lytic cocktail inhibited the production of the UCP1 in the RE + lytic group (blue arrows). (E): Quantitative analysis of immunohistochemistry staining of UCP1 in iWAT. Data were represented as means ± SD, n = 3 in each group, one-way ANOVA comparing UCP1 scores, ***$p < 0.001$.

There were more mitochondria in adipocytes and the mitochondria were tightly packed in the cytoplasm. Compared to the RE group, RE + lytic group was observed decreased number of mitochondria in the iWAT (Figure 5C 5.67 ± 0.47 versus 14.33 ± 1.70 per cell) and larger fat droplets continuously.

UCP1 is specifically expressed in the inner membrane of mitochondria of brown adipose cell. Increased UCP1 expression may cause hypermetabolism after burns, as was shown in immunohistochemistry in burn animals [26]. In Ctrl rats, there was no significant expression of UCP1 in iWAT, while UCP1 expression increased five-fold in mitochondria in RE rats (Figure 5D, E). These results showed that iWAT browning is related to burn-induced hypermetabolism through increased biogenesis of mitochondria and increased expression of UCP1. Similar to the Ctrl, UCP1 expression in iWAT in RE + lytic rats was significantly less than that of RE animals (Figure 5E). This indicates that lytic cocktail treatment alleviated burn-induced hypermetabolism through inhibition of the expression of UCP1 in browning of iWAT at a molecular and morphological level.

3.6. Lytic cocktail decreases the expression of thermogenesis related proteins and genes so as to inhibit iWAT browning

To further investigate the inhibitory effect of the lytic cocktail on adipose browning after burn injury, we examined the expression levels of the two main regulators of UCP1: PPAR-γ and PGC-1α in the iWAT. The results showed that the expression of UCP1 in the RE group was 1.7-fold ($p < 0.0001$) higher than the Ctrl and in the RE + lytic group it is 1.2-fold($p < 0.0001$) higher compared to Ctrl. The expression of PPAR-γ in the RE group was 2.2-fold ($p < 0.0001$) higher than Ctrl while in the RE + lytic group only 1.5-fold ($p < 0.0001$) higher than the Ctrl group. The expression of PGC-1α in the RE group was 2.4-fold higher than Ctrl while there is no big change (1.2-fold increase, N.S) in the RE + lytic group compared to Ctrl (Figure 6A, B). The results confirmed that the burn injuries increase the expression of UCP1, PGC-1α and PPAR-γ in iWAT, and the application of lytic cocktail to burn injuries reduces the production of these proteins.

These findings are also supported by the result of *Prdm16*, expression in different groups. In the RE group, mRNA expression of *Prdm16*, a transcription factor that activates brown adipose-specific genes, was 7-fold higher than that of the RE + lytic group (Figure 6C, $p < 0.001$). Likewise, *Tmem26* as a marker of beige adipocytes was upregulated in the iWAT of RE group. The expression of *Tmem26* of the RE was 1.2-fold higher than that of the RE + lytic (Figure 6D). Similarly, *Creb,* a downstream protein of a β-adrenergic receptor and a regulator of PGC-1α was upregulated in the iWAT of the RE group being 2.2-fold that of the RE + lytic group (Figure 6E).

4. Discussion

Previous studies have shown that the lytic cocktail can reduce catecholamine hormones within 24 h [11, 23]. Lytic cocktail modulates endocrine function indirectly, however, the specific target needs to be investigated. Currently, there is no confirmed evidence that shows lytic cocktails are effective against hypermetabolic states. According to our

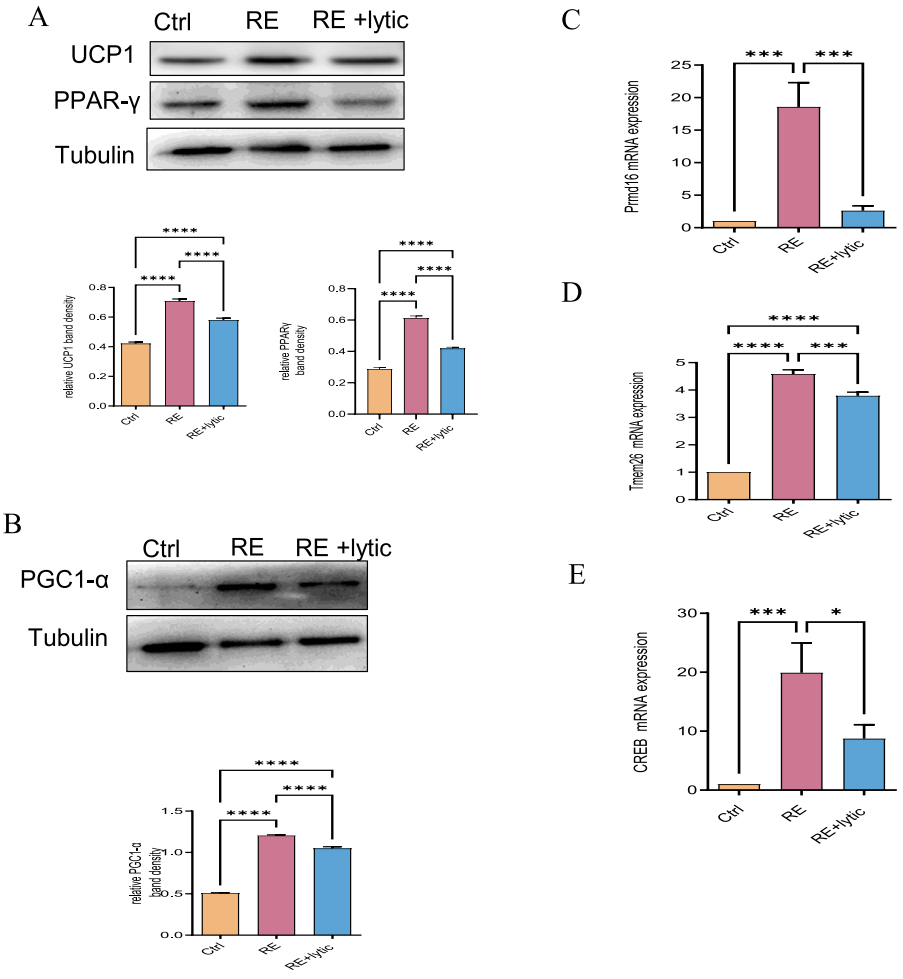

Figure 6. Molecular evidence of lytic cocktail's ability to reduce the expression of UCP1、PPAR-γ、PGC1-α in iWAT. Expressions of UCP1, PPAR-γ (A), PGC1-α (B) were analyzed by Western Blot in the three groups in six weeks after scalding. Lytic cocktail could reduce the expressions of these heat genetic proteins efficiently. Data were obtained from 9 beige adipose (n = 3 in each group) and was shown as the mean ± SD. One-way ANOVA comparing relative band density of UCP1, Par and PGC1-α. ****$p < 0.0001$. Expressions (fold change) of Prdm16 (C), Tmem26 (D) and Crab (E) of adipose were analyzed by PCR in Ctrl, RE and Realistic at 6 weeks after scalding. Data were obtained from 9 beige adipose (n = 3 in each group), and shown as the mean ± SD, One-way ANOVA comparing mRNA expression of Prmd16, Tmem26 and CREB, *$p < 0.05$, (***$p < 0.001$, ****$p < 0.0001$.

research noradrenaline and adrenaline were reduced and sustained in the relatively lower level after using lytic cocktail for 6 weeks, which indicates lytic cocktail not only can regulate the endocrine system especially stress hormone but also maintain such suppression in a period of time. We have provided evidence of proteomics results to verify that nuclear hormone receptor binding proteins and hormone receptor binding proteins are increased after using lytic cocktail.

Increased basal metabolic rates following burns is related to higher levels of catecholamines, renin, and angiotensin [4, 27]. Cytokines, glucocorticoids, endotoxin, reactive oxygen species, coagulation as well as complement cascades were believed to participate in the cascade of events following burn injuries [28], leading to a shifts in the body's metabolism of glucose, lipids, and amino acids [29, 30]. These factors act on numerous tissues and organs, including adipose tissue, leading to a hypermetabolic state in burn patients [27, 31, 32]. This is consistent with the rat burn model in our research. We observed that the rats in the Ctrl group had more food intake and higher body weight gain than the other two groups of scalded rats at one-week after scalding. The exceeding of Ctrl group indicated that the burn rats were already in a high consumption state. The metabolic behavior is inconsistent with what we observed in the levels of noradrenaline and adrenaline. Both hormone concentrations of the RE + lytic group were lowest at week 2. At week 2, the food intake of rats in the RE group was significantly higher than that in the RE + lytic group, while there was no significant difference in body weight gain between those two treated groups, indicating that the lytic cocktail can effectively improve the state of high consumption of the scalded rats.

Activated BAT has been recognized as the one of the culprits for the increased energy expenditure [33], and it is activated by the sympathetic nervous system [34, 35]. Some research reported that browning happens 5–6 days after burn [18, 35], other researchers reported that it might take up to 20 days [26]. In order to study if lytic cocktail could alleviate hypermetabolism for a longer time period, we harvested the adipose tissue at 6 weeks after trauma. ^{18}F-FDG-PET/CT is an effective way to assess the metabolism of a specific tissue [36, 37], and high ^{18}FDG uptake could manifest the accurate localization of browning WAT [38]. Glucose uptake is increased in BAT after injection of noradrenaline in rats [39]. Serum norepinephrine increased dramatically after severe burn. It has been proved that glucose utilization in BAT dependences on the serial activation of UCP1 and AMP kinase [40]. Therefore, ^{18}F-FDG-PET/CT can reflect the metabolism of browning white adipose.

Studies have shown that intake of ^{18}FDG by BAT could be increased due to burn stimulation [41]. Different parts in the rat's body of WAT vary in their biological characteristics, such as protein content, metabolic enzyme activity, and its propensity to transdifferentiate into beige fat [42]. iWAT may rapidly be converted into beige fat upon adrenaline stimulation [43], so we focused on metabolic rate in iWAT. Our study confirmed that the uptake of ^{18}FDG of iWAT is increased after burns, proving that iWAT metabolism may be increased. In our experiment, the lytic cocktails effectively reduced the uptake of ^{18}FDG which indicates the inhibition of the metabolic rate of iWAT.

Considering the development in proteomics, the direct assessment of the proteins in iWAT appears as a practical approach to obtain the protein difference between RE and RE + lytic groups. Gene Ontology analysis provide information linking genes and proteins. As a tool, it provides the most comprehensive information annotation and classification services for all proteins in the project. According to the result of GO analysis, the expression of the metabolic related proteins in iWAT indeed decreased after applying lytic cocktail, it indicated that metabolic prohibition of lytic cocktail is concerned with reducing expression of thermogenic proteins.

White adipose subjected to persistently elevated catecholamine levels, changes its morphology and function: the intracellular fat vacuole shrinks while the number of mitochondria increases. Along with the increasing expression of UCP-1 mRNA and protein, white adipose is transdifferentiated into a heat-generating beige adipose. Another mediator involved in the adipose transdifferentiation is a nuclear receptor PPAR-γ and a transcription factor PGC-1α, both of which regulate the browning process [44]. PGC-1α, one of the main regulators of fatty acid oxidation, is essential for thermogenesis [45]. PPAR-γ controls the general process of adipogenesis in all fat lineages and regulates brown fat-specific characteristics [46].

Previous research has revealed historical changes in WAT after burn injuries [35, 43, 47]. Our research further investigated these changes in iWAT by H&E, TEM, and immunohistochemistry of UCP1 which is the most widely used brown adipocyte-specific marker. The results confirmed that burn injuries could result in increasing the numbers of iWAT mitochondria, while the lytic cocktail treatment inhibited the thermogenic and morphological changes in the RE + lytic group. In this study, the Western blot analysis results provided further evidence that iWAT browning is responsible for burn injury-induced hypermetabolic state. The metabolic rate of burn animals decreased after treatment by lytic cocktail. Compared to the RE, the reduced food consumption in the RE + lytic group was associated with the reduction of iWAT browning and inhibition of UCP1 expression.

This study showed that there are higher expressions of *Tmem26* (a marker of beige fat) after burns and lower expressions of PGC-1α, PPAR-γ and *Prdm16* in the RE + lytic group. Lytic cocktail may suppress the expression of PPAR-γ and PGC-1α by inhibiting *Prdm16*, downregulating the expression of UCP1. Lytic cocktail decreases the expression of those critical molecules that regulate the function of UCP1, while UCP1 influences the glucose metabolism, which further inhibits the hypermetabolism after severe burns. The inhibitory function of lytic cocktail on hypermetabolic state may be related to decreased circulating norepinephrine and adrenaline levels.

In conclusion, in this paper we confirmed that lytic cocktail could inhibit the WAT browning, decrease energy consumption, and ultimately reduce the hypermetabolism in severe burn rats. Our study found that these effects could be caused by the decreased expression levels of plasma norepinephrine and epinephrine that are regulated by the application of lytic cocktail. We have proved that lytic cocktail inhibits white adipose tissue browning and restrains hypermetabolism via reducing circulating stress hormone levels. Those findings suggested that beside being used as a sedation method, the lytic cocktail medicines might be a promising treatment for alleviation of hyper-metabolism induced by severe burns or trauma in clinics.

Declarations

Author contribution statement

Meng Zhang: Conceived and designed the experiments; Performed the experiments; Analyzed and interpreted the data; Contributed reagents, materials, analysis tools or data; Wrote the paper.

Peilang Yang: Conceived and designed the experiments; Analyzed and interpreted the data; Contributed reagents, materials, analysis tools or data.

Tianyi Yu: Conceived and designed the experiments; Analyzed and interpreted the data.

Martin C Harmsen: Analyzed and interpreted the data; Wrote the paper.

Min Gao; Dan Liu; Yan Shi: Analyzed and interpreted the data.

Yan Liu; Xiong Zhang: Conceived and designed the experiments; Contributed reagents, materials, analysis tools or data; Wrote the paper.

Funding statement

This work was supported by National Natural Science Foundation of China [81270909]; Research Grant from Shanghai Hospital Development Center [SHDC12014117]; Shanghai Collaborative Innovation Center for Translational Medical [TM201705]; and the National Natural Science Foundation of China [81871564].

Data availability statement

Data included in article/supplementary material/referenced in article.

Declaration of interests statement

The authors declare no conflict of interest.

Additional information

Supplementary content related to this article has been published online at https://doi.org/10.1016/j.heliyon.2022.e09128.

References

[1] F.N. Williams, D.N. Herndon, M.G. Jeschke, The hypermetabolic response to burn injury and interventions to modify this response, Clin. Plast. Surg. 36 (4) (2009) 583–596.
[2] I. Kaddoura, et al., Burn injury: review of pathophysiology and therapeutic modalities in major burns, Ann. Burns Fire Dis. 30 (2) (2017) 95–102.
[3] W.B. Norbury, et al., Urinary cortisol and catecholamine excretion after burn injury in children, J. Clin. Endocrinol. Metab. 93 (4) (2008) 1270–1275.
[4] M.G. Jeschke, et al., Long-term persistance of the pathophysiologic response to severe burn injury, PLoS One 6 (7) (2011), e21245.
[5] M.G. Jeschke, Postburn hypermetabolism: past, present, and future, J. Burn Care Res. 37 (2) (2016) 86–96.
[6] A. Clark, et al., Nutrition and metabolism in burn patients, Burns Traum. 5 (2017) 11.
[7] C. Price, Nutrition: reducing the hypermetabolic response to thermal injury, Br. J. Nurs. 27 (12) (2018) 661–670.
[8] J. Meunier-Cartal, J.C. Souberbielle, F. Boureau, Morphine and the "lytic cocktail" for terminally ill patients in a French general hospital: evidence for an inverse relationship, J. Pain Symptom Manag. 10 (4) (1995) 267–273.
[9] I.Z. Yardeni, et al., Comparison of postoperative pain management techniques on endocrine response to surgery: a randomised controlled trial, Int. J. Surg. 5 (4) (2007) 239–243.
[10] L. Berntman, C. Carlsson, Influence of "lytic cocktail" on blood flow and oxygen consumption in the rat brain, Acta Anaesthesiol. Scand. 22 (5) (1978) 515–518.
[11] S. Wang, et al., [An experimental study on the influence of inhibition of postburn stress on inflammatory reaction in severely scalded rats], Zhonghua Shaoshang Zazhi 18 (5) (2002) 268–271.
[12] Q.B. Shao, et al., [Protective effect of early application of lytic cocktail on small intestine of severely scalded rats], Zhonghua Shaoshang Zazhi 26 (3) (2010) 180–184.
[13] L.S. Sidossis, et al., Browning of subcutaneous white adipose tissue in humans after severe adrenergic stress, Cell Metabol. 22 (2) (2015) 219–227.
[14] K. Yo, et al., Brown adipose tissue and its modulation by a mitochondria-targeted peptide in rat burn injury-induced hypermetabolism, Am. J. Physiol. Endocrinol. Metab. 304 (4) (2013) E331–E341.
[15] A. Giordano, et al., Presence and distribution of cholinergic nerves in rat mediastinal brown adipose tissue, J. Histochem. Cytochem. 52 (7) (2004) 923–930.
[16] A. Giordano, et al., White, brown and pink adipocytes: the extraordinary plasticity of the adipose organ, Eur. J. Endocrinol. 170 (5) (2014) R159–R171.
[17] M.R. Boon, W.D. van Marken Lichtenbelt, Brown adipose tissue: a human perspective, Handb. Exp. Pharmacol. 233 (2016) 301–319.
[18] A. Abdullahi, et al., IL-6 signal from the bone marrow is required for the browning of white adipose tissue post burn injury, Shock 47 (1) (2017) 33–39.
[19] A.M. Bertholet, Y. Kirichok, UCP1: a transporter for H(+) and fatty acid anions, Biochimie 134 (2017) 28–34.
[20] Y.M. Yu, et al., The metabolic basis of the increase of the increase in energy expenditure in severely burned patients, JPEN - J. Parenter. Enter. Nutr. 23 (3) (1999) 160–168.
[21] Y. Chen, et al., Thermal stress induces glycolytic beige fat formation via a myogenic state, Nature 565 (7738) (2019) 180–185.
[22] A. Mulya, J.P. Kirwan, Brown and beige adipose tissue: therapy for obesity and its comorbidities? Endocrinol Metab. Clin. N. Am. 45 (3) (2016) 605–621.
[23] D. Patsouris, et al., Burn induces browning of the subcutaneous white adipose tissue in mice and humans, Cell Rep 13 (8) (2015) 1538–1544.
[24] U.S. Dinish, et al., Diffuse optical spectroscopy and imaging to detect and quantify adipose tissue browning, Sci. Rep. 7 (2017) 41357.
[25] Z. Guo, et al., TELO2 induced progression of colorectal cancer by binding with RICTOR through mTORC2, Oncol. Rep. 45 (2) (2021) 523–534.
[26] C. Porter, et al., Severe burn injury induces thermogenically functional mitochondria in murine white adipose tissue, Shock 44 (3) (2015) 258–264.
[27] D.N. Herndon, et al., Reversal of catabolism by beta-blockade after severe burns, N. Engl. J. Med. 345 (17) (2001) 1223–1229.
[28] R.L. Sheridan, A great constitutional disturbance, N. Engl. J. Med. 345 (17) (2001) 1271–1272.
[29] N. Ballian, et al., Glucose metabolism in burn patients: the role of insulin and other endocrine hormones, Burns 36 (5) (2010) 599–605.
[30] R. Kraft, et al., Association of postburn fatty acids and triglycerides with clinical outcome in severely burned children, J. Clin. Endocrinol. Metab. 98 (1) (2013) 314–321.
[31] D.W. Hart, et al., Determinants of skeletal muscle catabolism after severe burn, Ann. Surg. 232 (4) (2000) 455–465.
[32] R. Kraft, et al., Occurrence of multiorgan dysfunction in pediatric burn patients: incidence and clinical outcome, Ann. Surg. 259 (2) (2014) 381–387.
[33] B.S. Finlin, et al., Human adipose beiging in response to cold and mirabegron, JCI Insight 3 (15) (2018).
[34] J.E. Silva, S.D.C. Bianco, Thyroid-adrenergic interactions: physiological and clinical implications, Thyroid : Off. J. Am. Thyr. Ass. 18 (2) (2008) 157–165.
[35] A. Abdullahi, et al., Alternatively activated macrophages drive browning of white adipose tissue in burns, Ann. Surg. 269 (3) (2019) 554–563.
[36] A.M. Cypess, et al., Identification and importance of brown adipose tissue in adult humans, N. Engl. J. Med. 360 (15) (2009) 1509–1517.
[37] M.R. Mirbolooki, et al., Quantitative assessment of brown adipose tissue metabolic activity and volume using 18F-FDG PET/CT and β3-adrenergic receptor activation, EJNMMI Res. 1 (1) (2011) 30.
[38] J.W. Park, et al., 18F-FDG PET/CT monitoring of beta3 agonist-stimulated brown adipocyte recruitment in white adipose tissue, J. Nucl. Med. 56 (1) (2015) 153–158.
[39] G.J. Cooney, I.D. Caterson, E.A. Newsholme, The effect of insulin and noradrenaline on the uptake of 2-[1-14C]deoxyglucose in vivo by brown adipose tissue and other glucose-utilising tissues of the mouse, FEBS Lett 188 (2) (1985) 257–261.
[40] K. Inokuma, et al., Uncoupling protein 1 is necessary for norepinephrine-induced glucose utilization in brown adipose tissue, Diabetes 54 (5) (2005) 1385–1391.
[41] A. Vegiopoulos, et al., Cyclooxygenase-2 controls energy homeostasis in mice by de novo recruitment of brown adipocytes, Science 328 (5982) (2010) 1158–1161.
[42] F. Zhang, et al., An adipose tissue atlas: an image-guided identification of human-like BAT and beige depots in rodents, Cell Metabol. 27 (1) (2018) 252–262, e3.
[43] E.A. Carter, et al., Effects of burn injury, cold stress and cutaneous wound injury on the morphology and energy metabolism of murine brown adipose tissue (BAT) in vivo, Life Sci 89 (3-4) (2011) 78–85.
[44] T. Montanari, N. Pošćić, M. Colitti, Factors involved in white-to-brown adipose tissue conversion and in thermogenesis: a review, Obes. Rev. 18 (5) (2017) 495–513.
[45] T. Goto, et al., The hepatokine FGF21 is crucial for peroxisome proliferator-activated receptor-alpha agonist-induced amelioration of metabolic disorders in obese mice, J. Biol. Chem. 292 (22) (2017) 9175–9190.
[46] N. Petrovic, et al., Chronic peroxisome proliferator-activated receptor gamma (PPARgamma) activation of epididymally derived white adipocyte cultures reveals a population of thermogenically competent, UCP1-containing adipocytes molecularly distinct from classic brown adipocytes, J. Biol. Chem. 285 (10) (2010) 7153–7164.
[47] M. Chondronikola, et al., Brown adipose tissue improves whole-body glucose homeostasis and insulin sensitivity in humans, Diabetes 63 (12) (2014) 4089–4099.